Optics & Laser Technology 135 (2021) 106691

Contents lists available at ScienceDirect

Optics and Laser Technology

journal homepage: www.elsevier.com/locate/optlastec

Full length article

Kramers-Kronig analysis of the optical linearity and nonlinearity of nanostructured Ga-doped ZnO thin films

H. Elhosiny Ali [a,c,*], V. Ganesh [a], L. Haritha [b], A.M. Aboraia [d,e], H.H. Hegazy [a,e], V. Butova [d], Alexander V. Soldatov [d], H. Algarni [a], A. Guda [d], H.Y. Zahran [a,f], Yasmin Khairy [c,*], I.S. Yahia [a,f,g]

[a] Advanced Functional Materials & Optoelectronic Laboratory (AFMOL), Department of Physics, Faculty of Science, King Khalid University, P.O. Box 9004, Abha, Saudi Arabia
[b] Department of Physics, Telanga University, Nizamabad, Telangana 503322, India
[c] Physics Department, Faculty of Science, Zagazig University, Zagazig 44519, Egypt
[d] The Smart Materials Research Institute, Southern Federal University, Sladkova 178/24, 344090 Rostov-on-Don, Russia
[e] Department of Physics, Faculty of Science, Al-Azhar University, Assiut 71542, Egypt
[f] Nanoscience Laboratory for Environmental and Bio-medical Applications (NLEBA), Semiconductor Lab., Metallurgical Lab.1, Physics Department, Faculty of Education, Ain Shams University, Roxy 11757, Cairo, Egypt
[g] Research Center for Advanced Materials Science (RCAMS), King Khalid University, Abha 61413, P.O. Box 9004, Saudi Arabia

ARTICLE INFO

Keywords:
Ga-doped ZnO
Nanostructured thin films
Sol-gel/spin coating technique
Bandgap analysis
Linear/nonlinear optical parameters

ABSTRACT

Pure zinc oxide and gallium-doped ZnO films have been deposited on a glass substrate using a sol-gel assisted spin coating technique. The prepared films were characterized by structural, morphological, optical, and the effect of doping is studied. XRD analyses of the films confirm amorphous nature. Raman studies give support to XRD and confirm secondary phases are absent in the film. The AFM images give the grain size, which decreases with an increase in doping concentration from 116 nm to 81 nm. Roughness, Skewness, and Kurtosis factor are varying from 45.694 nm to 29.153 nm 1.085 to 0.453, 3.583 to 2.605, respectively. Kramers-Kronig equations are the most accurate methodology for optical thin-film technology for the calculations of optical linearity and nonlinearity parameters. The bandgap values are decreasing with increasing thickness from 2.97 to 2.79, respectively. The doped films are more transparent compared to the pure ZnO films. The enhancement in the linear optical properties such as refractive index, absorption index, and dielectric constant are also observed with an increase in the doping concentration. The nonlinear optical properties such as $\chi^{(1)}$, $\chi^{(3)}$ and $n^{(2)}$ are varying in the range of 0.288 esu to 0.252 esu, 1.1×10^{-12} esu to 7×10^{-13} esu, 1.92×10^{-11} esu to 1.30×10^{-11} esu, respectively. The enhancement in optical properties with increasing the doping concentration suggests the present films are useful for various optical device applications.

1. Introduction

In the recent past, there is a considerable demand for the synthesis of transitions metal oxide thin films as they possess potential applications in various fields such as gas sensors materials [1], electrochromic films [2], catalysts, electrodes, acoustic wave devices, etc. [3–9]. Amongst all the metal oxide, ZnO is a promising candidate due to its potential applications in optoelectronics and electronic devices. ZnO also possesses several properties like thermal stability, low-cost, high resistance to chemical attack, lower toxicity [10,11], and suitable adhesive with several substrates [12]. Furthermore, ZnO is an n-type semiconductor with wide bandgap (3.37 eV) and low resistivity, making it convenient to use transparent electrodes in electronic displays [13].

Almost all the available techniques have been adopted to deposit pure and doped-ZnO films. Chemical vapor deposition technique [14], pulsed laser deposition [15], RF-magnetron sputtering [16], molecular beam epitaxy [17], chemical spray pyrolysis [18] yields a good quality film. Here in the present study, we have adopted the sol-gel assisted spin coating technique to deposit the ZnO films. To improve the optical and electrical properties of the films, doping is an effective favorable technique adopted by many researchers and been successful [19,20]. To enhance the properties of the films, the researchers have focused on varying the deposition techniques, annealing the films at different temperatures, doping with suitable elements. Dopants such as Al-, Cu-,

* Corresponding authors at: Physics Department, Faculty of Science, Zagazig University, Zagazig 44519, Egypt.
E-mail addresses: hitham_ph@gmail.com (H. Elhosiny Ali), yasmin_ph@zu.edu.eg (Y. Khairy).

https://doi.org/10.1016/j.optlastec.2020.106691
Received 11 February 2020; Received in revised form 11 July 2020; Accepted 15 October 2020
Available online 1 November 2020
0030-3992/

Sn-, Cd-, Ag- have been doped in ZnO films [19,20], and the properties have been studied extensively. ZnO is an n-type material consisting of dominant Zinc interstitials, oxygen vacancies that generate donor levels [21,22]. Among all the dopants, Gallium is attracted many researchers due to its potential applications in the field of UV-detectors, optoelectronic, TCO, and bandgap narrowing for photoelectron, nonlinear optical applications [23–26]. It is also an n-type dopant which controls the n-type electrical conductivity in ZnO material, and useful for optoelectronic applications.

There are many reports available on Ga-doped thin films in the literature, but in the filed systematical study of nonlinear optical properties is still lacking. Especially in Kramers-Kronig calculations of optical constant, there very few reports are reported until now [27]. Kramers-Kronig dispersion relations are the most useful for accurate calculation of the optical parameters like refractive index and absorption index from reflectance data. Thus, it is worthwhile to calculate the optical linear and nonlinear properties of Ga-doped ZnO films Viz., Kramers-Kronig relation. To the best of our knowledge, this is the first report work to calculate the optical parameters of Ga: ZnO thin films using Kramers-Kronig relations. The detailed study is discussed in successive parts.

2. Experimental details

2.1. Synthesis of Ga-doped ZnO nanostructured films.

The films of pure ZnO and Ga-doped ZnO were deposited on the glass substrate by the sol-gel assisted spin-coating technique. All the chemicals used in the preparation process are of analar grade and purchased from Sigma-Aldrich. The starting solution is of 0.2 M concentration Zinc acetate dehydrate dissolved in 2-methoxyphenyl and continuously stirred at 60 °C for 1 h. Monoethanolamine (MEA), as the complexing agent, and stabilizer are added to the solution maintaining the molar ratio MEA/Zn as 1. To obtain the homogeneous mixture, the solution is continuously stirred for an hour and thus obtained a clear solution is termed as a -sol. Gallium nitrate is used as the source of dopant and added in stoichiometric quantities to prepare the Ga-doped ZnO films. The glass substrates were cleaned with distilled water, followed by an isopropanol solution. Thus, the preapared solution is used to coat the films using the spin coater at a speed of 1500 rpm, same procedure is repeated for the coating of ten layers. After the coating is completed, the substrates will dry at 125 °C and for 10 min between each layer. All the doped films are prepared similarly. The final films will be subjected to annealing at 450 °C temperature inside the muffle furnace to have the nanostrctured Ga-doped ZnO samples. Further, the thickness of the films were measured using thickness monitor instrument.

2.2. Devices and measurements.

The structural characteristics of Ga-doped and pure ZnO thin films were investigated using the X-ray diffractometer (Shimadzu LabX, wavelength 6000) with monochromatic CuK_{α} source operated at 30 kV and 25 mA.

The surface morphologies and its related parameters, i.e., the grain sizes of the pure and Ga-doped ZnO films, were studied by the Atomic force microscope (AFM). (Solver next Russia)

Raman spectrometer (TS, DXR) is used in 200–1400 cm^{-1} to obtain information about secondary phases and vibrational modes inside the studied samples.

Transmittance, reflectance, and absorbance measurements were measured using the JASCO UV–VIS-NIR-570 spectrophotometer in the range from 290 to 1000 nm.

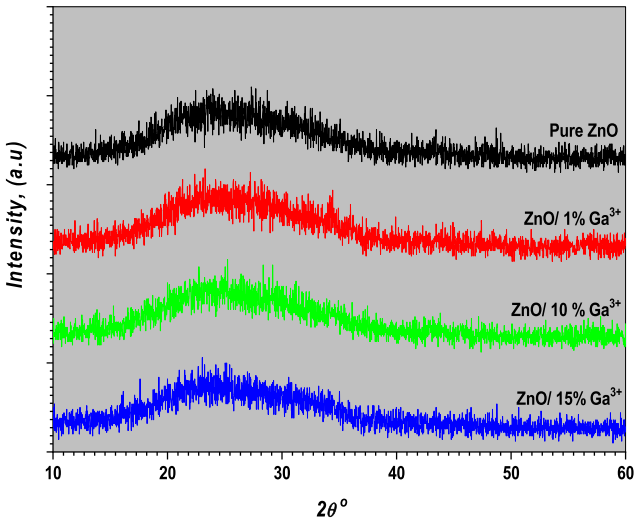

Fig. 1. XRD patterns of pure and Ga: ZnO nanostructured thin films.

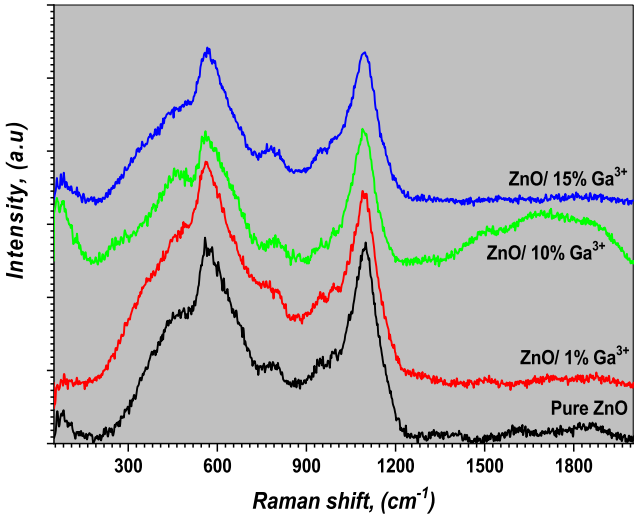

Fig. 2. Raman spectra of pure and Ga: ZnO nanostructured thin films.

3. Results and discussions

3.1. XRD measurements of nanostructured Ga-doped ZnO films

The X-ray diffraction studies of pure, and 1%, 10%, 15% Ga-doped ZnO thin films are depicted in Fig. 1. It is inferred that all the films deposited are amorphous. The broad hump in all the samples indicates the nanostructured nature of the present samples [27]. There is a small peak observed at 34° in 1% Ga-samples. The intensity of the peak is decreased with higher doping concentration and become amorphous. The reason for this type of nature is attributed to occupation of the Ga^{+3}-ions occupy the site of $Zn^{2+}$and higher ionic radius of Ga^{+3} ions ompare to Zn^{2+} ions. Reza Ebrahimifard et al. have studied Al-Ga co-doped ZnO thin films, and they concluded in their detail study that at higher concentration of doping atoms occupy the interstitial positions or form Al- and Ga- oxides (more than 5%), which entirely distort ZnO crystal structure [24]. Shuqun Chen et al. also explained the reason for decreasing crystallinity at higher concentration of Ga-doped ZnO is due to increase the segregation of extra Ga-atoms at grain boundaries suppresses the grain growth and, the films are thickened by isolated particles resulting the crystal quality is reduced [28]. The detail explanation

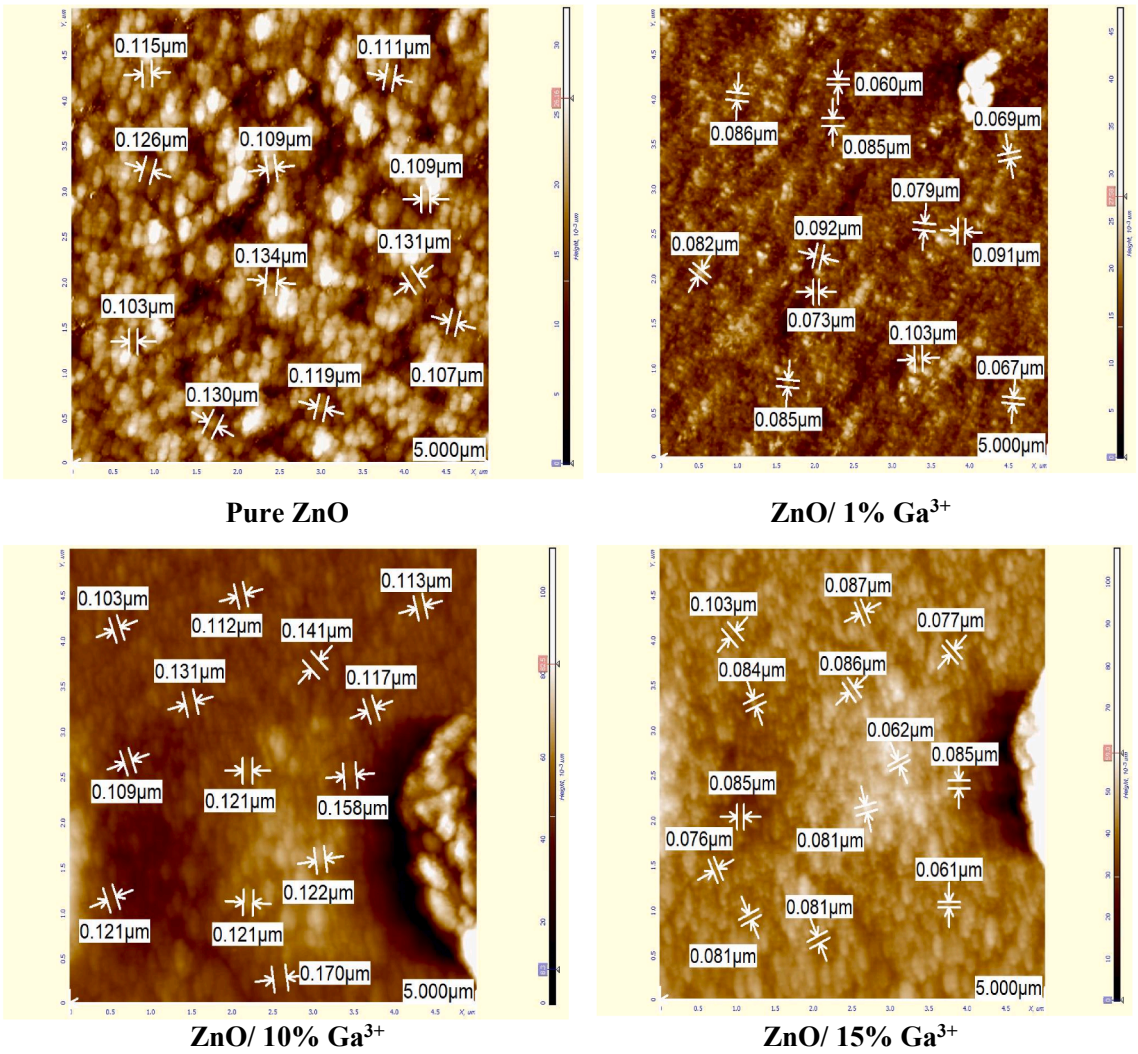

Fig. 3. AFM images of pure and Ga: ZnO nanostructured thin films.

Table 1
Surface morphological, grain size analysis and roughness analysis of nanostructured Ga-doped ZnO thin films.

Materials	Mean The mean values of the grain Size, (nm)	Ra, The arithmetical mean deviation of the profile	Rq, Root-mean-square deviation of the profile	Rsk, Skewness of profile	Rku, Kurtosis of profile
Pure Zno	116 nm	45.694	60.169	1.085	3.583
ZnO/1% Ga	111 nm	24.068	29.702	0.287	2.610
ZnO/10% Ga	126 nm	19.517	22.713	0.448	2.480
ZnO/15% Ga	81 nm	29.153	36.189	0.453	2.605

about the amorphous nature of present samples and with some other dopants was explained in earlier studies [24,27]

3.2. Raman analysis of nanostructured Ga-doped ZnO films

The modes of vibrations of pure ZnO and Ga-doped ZnO films are shown in Fig. 2. The peaks are observed at 100, 273, 330, 435, and 580 cm^{-1}, indeed correspond to the optical and acoustic modes of vibration. The peaks centered at 100 and 435 cm^{-1} are attributed to doubly degenerate acoustic and optical modes, respectively. The peaks at 273 cm^{-1} and 332 cm^{-1} correspond to the singly degenerate acoustic vibrational mode and transverse optical mode, whereas the peak at 583 cm^{-1} corresponds to longitudinal optical mode. The shift in the peaks and broadening of the peaks is due to the doping of Ga-, which may be the reason behind defects and oxygen vacancies. Similar behavior is observed on pure and Al-, Fe-, Sb-doped ZnO thin films [29–32].

3.3. Morphology study of nanostructured Ga-doped ZnO films

It is well known that the films optical and electrical properties are connected with the grain size. Hence, it is worthwhile to look at the morphology of Ga-doped and pure ZnO films. Thus, the AFM images are

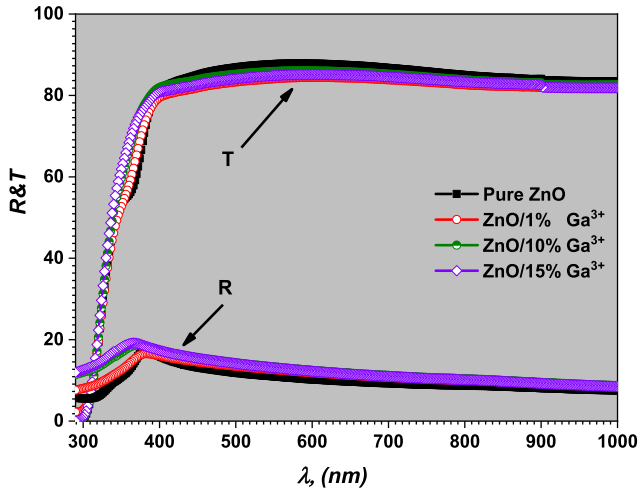

Fig. 4. Transmission and reflectance spectra plots as a function of wavelength for pure and Ga: ZnO nanostructured thin films.

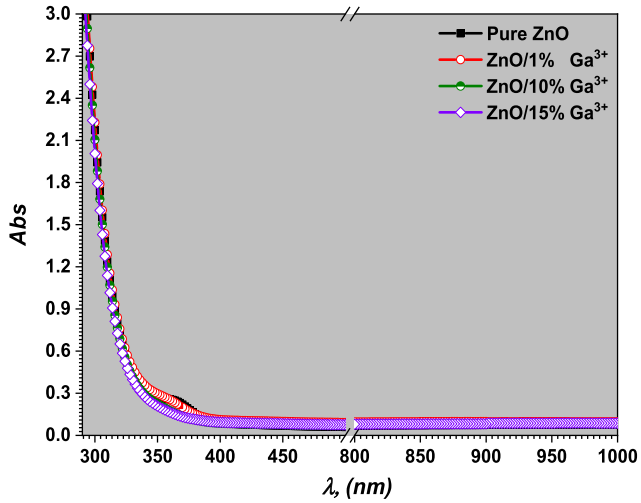

Fig. 5. Absorption spectra plots as a function of wavelength for pure and Ga: ZnO nanostructured thin films.

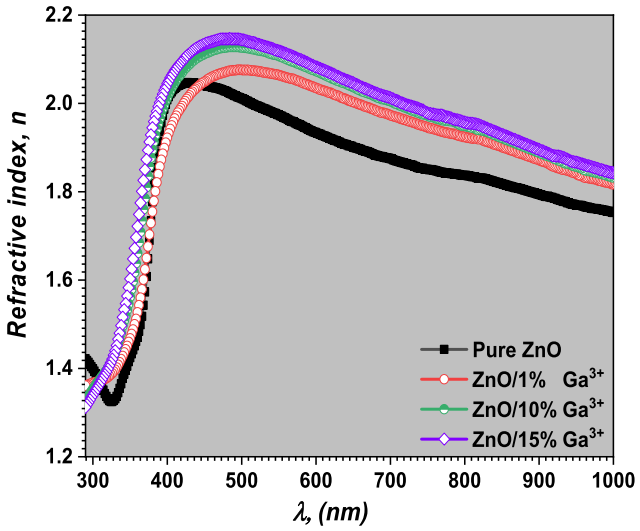

Fig. 6. Refractive index plots as a function of wavelength for pure and Ga: ZnO nanostructured thin films.

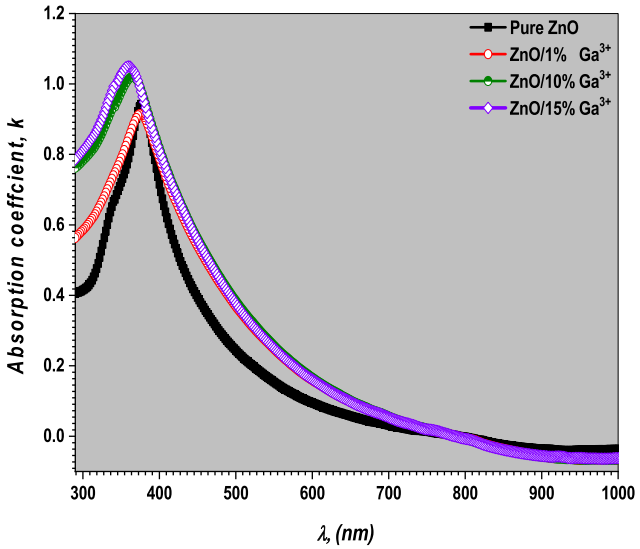

Fig. 7. absorption coefficient plots as a function of wavelength for pure and Ga: ZnO nanostructured thin films.

depicted in Fig. 3, from which the grain size is evaluated. Moreover, it is observed that the grains are spherical. The grain size and roughness decrease with an increase in the concentration of doping Ga- in ZnO films is attributed to the effect of doping and increases the quality of the film. Some other properties like Skewness and Kurtosis factor are also studies to understand the quality of the prepared films. The values of roughness Skewness and Kurtosis factor varying from 45.694 nm to 29.153 nm 1.085 to 0.453, 3.583 to 2.605, respectively are given in Table 1. A similar type of results is observed in previously reported data [27].

3.4. Linear optical analysis of nanostructured Ga-doped ZnO thin films

Fig. 4. represents the optical transmittance and reflectance spectra in the range of 290–1000 nm for pure and Ga- (1–15%) doped ZnO samples. It is evident from the figure that all the films are highly transparent in the visible region, and its average is found to be around 80–90%. As explained earlier, doping of Ga- on to ZnO films inhibits the transmittance of the films, i.e., the transmittance decreases slightly on doping, which may be attributed to the change in grain size as observed in the AFM images. The increase in the doping transmittance is observed for the doped film, which is in correlation with our previously reported data of Rhodamine B dye and Rose Bengal thin films [21,27,29]. The increase in transmittance and a decrease in reflectance of Ga: ZnO thin films indicate the present films are useful for optoelectronic applications.

The absorbance edge increase with the doping concentration of Ga-, moreover the absorption shows (Fig. 5) a bump in the UV-region than in visible region, which is making these films to have application in many optoelectronic devices. Similar behavior is absorbed for many oxide films like CdO, NiO, etc in several reports [33,34].

The key parameters in deciding the quality and nature of optoelectronic devices are Refractive index n and extinction coefficient k. These parameters are evaluated from the Kramers-Kronig method by using the given equations [35] for the whole wavelength range. The values of T and R are taken from Fig. 4 [29].

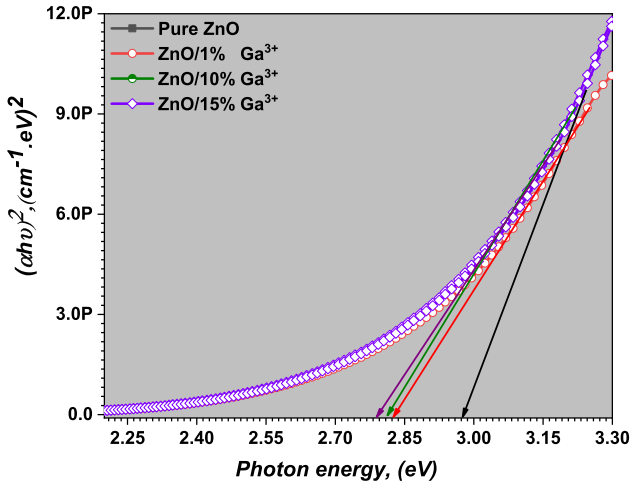

Fig. 8. Bandgap analysis for pure and Ga: ZnO nanostructured thin films.

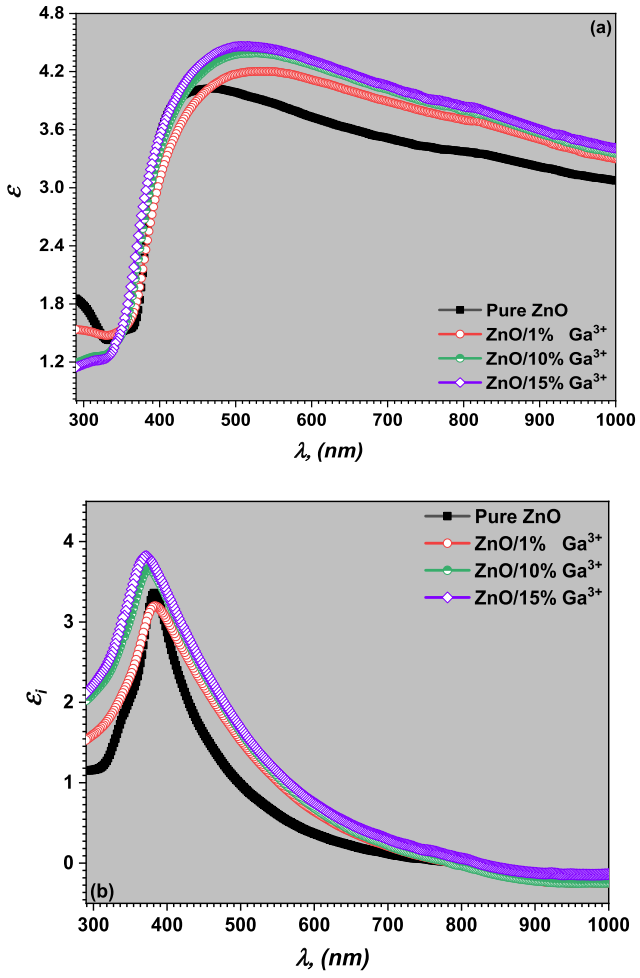

Fig. 9. (a, b) The variation of dielectric constant and dielectric loss as a function of wavelength for pure and Ga: ZnO nanostructured thin films.

$$n(\omega) = \frac{1 - R(\omega)}{1 + R(\omega) - 2\sqrt{R(\omega)}cos\phi(\omega)} \quad (1)$$

$$k(\omega) = \frac{2\sqrt{R(\omega)}sin\phi(\omega)}{1 + R(\omega) - 2\sqrt{R(\omega)}cos\phi(\omega)} \quad (2)$$

where

$$\phi(\omega) = \frac{-\omega}{\pi}\int_0^{\infty} \frac{\ln R(\omega') - lnR(\omega)}{\omega'^2 - \omega^2} d\omega' \quad (3)$$

The refractive index "n" as a function of wavelength is depicted in Fig. 6. The increase in the value of "n" is observed with an increase in Ga-concentrations. The minimum value of "n" is observed at a wavelength corresponding to $h\nu = E_g$. The absorption coefficient "k" an important optical constant calculated and is plotted as a function of wavelength. Similar to refractive index, the absorption coefficient also increases with increasing in the Ga-doping percentage (Fig. 7). Moreover, the value of "k" is very less at a higher wavelength, which indicates the films are highly transparent at higher wavelengths. A similar type of behavior is observed in our earlier reported data [27,29].

The absorption coefficient ($\alpha = 4\pi k/\lambda$) is calculated from the band to band transition, and it pursues the following condition [36]:

$$(\alpha E)^h = Q(E - E_g) \quad (4)$$

where E is the incident photon energy, E_g is the energy gap, Q is a bandgap constant. h is a constant which describes the electronic transition, and it takes value 2 for direct transition and 1/2 for the indirect transition. The variation of $(\alpha h\nu)^2$ as a function of $(h\nu)$, as shown in Fig. 8. It has been absorbed that the direct bandgap is decreasing with an increase in the concentration of Ga- in ZnO films. The decrease in the transmittance of the films results in the decrease of energy gap values, making these films suitbale for optoelectronic applications. The observed bandgap values are quite high from the previously reported of Kramers–Kronig approach of these films. This results are useful for optoelectronic device applications [27–29]

Knowing the values of n and k, the optical dielectric constants (real and imaginary parts) can be expressed from the following relations [37]

$$\varepsilon_r = n^2 - k^2 \quad (5)$$

$$\varepsilon_i = 2nk, \quad (6)$$

Fig. 9(a,b) showed the variation of dielectric constant and dielectric loss with wavelength. The dielectric values showed a peak at lower wavelengths and seemed to be constant for the higher wavelengths. Moreover, the low values of the dielectric constants in the range of 4.03–4.50 for all the doped films. The calculated optical parameters of the studied films are depicted in Table 2. From this table, it is clear that the optical parameters showed higher values than the earlier reported data of thin films. This indicating that the present Ga-dopant showing remarkable effect on ZnO for various device applications. The comparison data of present work and various other thin films are given in Table 3.

3.5. Nonlinear optical analysis of nanostructured Ga-doped ZnO thin films

When the films are exposed to high energy radiation like a laser, second and higher-order harmonics are generated. Thus at high intensities, the polarization is a non-linear function of an electric field, whereas linear function at low intensity. Therefore, it is necessary to

Table 2
Optical and dielectric parameters of analysis of nanostructured Ga-doped ZnO thin films.

Materials	Thickness, (nm)	Bandgap, (eV)	Refractive index, (n)	Absorption coefficient, (k)	ε_1	ε_2
Pure Zno	226	2.97	2.04	0.94	4.03	3.40
ZnO/1% Ga	227	2.82	2.08	0.91	4.22	3.24
ZnO/10% Ga	229	2.80	2.13	1.02	4.41	3.66
ZnO/15% Ga	228	2.79	2.15	1.05	4.50	3.87

Table 3
Comparative E_g and ε_1 and ε_2 values of previously reported optical parameters thin films by Kramers-Kronig analysis.

Authors	Material	E_g, (eV)	ε_1	ε_2
Aslam et al. (Optics and Laser Technology, 112 (2019) 207–214)	Rose Bengal	1.92–1979	4.03	3.40
Abutalib et al. [Optik, 127 (2016) 6601–6609]	Fluorescein dye	1.95–1.99	2.7–4.9	0.05–1.1
I.S. Yahia et al. [Physica B, 490 (2016) 25–30]	Rhodamine	2.10	0.02–5.5	–

study the variation of the first-order susceptibility $\chi^{(1)}$, third-order optical susceptibility $\chi^{(3)}$, and nonlinear refractive index n^2 as a function of wavelength. Hence enabling films for applications like communication system, optical signal processing, electro-optic modulators, optical circuits [38,39]. Thus the equations are calculated as follows [40–42]:

$$\chi^{(1)} = \frac{n_o^2 - 1}{4\pi} \tag{7}$$

$$\chi^{(3)} = A\left(\frac{n_o^2 - 1}{4\pi}\right)^4 \tag{8}$$

$$n^{(2)} = \frac{12\pi\chi^{(3)}}{n_0} \tag{9}$$

where A is a constant, and its value is 1.7×10^{-10} esu [28]. Fig. 10(a-c) gives the variation of $\chi^{(1)}$, $\chi^{(3)}$, and $n^{(2)}$ as a function of wavelength. It is understood that the nonlinear susceptibilities and non-linear refractive index behave similarly. The calculated values of $\chi^{(1)}$and $\chi^{(3)}$ are varying in the range of 0.288 to 0.252 and 1.1×10^{-12} esu to 7×10^{-13} esu, respectively. Similarly, the nonlinear refractive index varies in the range of 1.92×10^{-11} esu to 1.30×10^{-11} esu. The observed values of nonlinear optical parameters are quite higher than earlier reported data of other thin films [27,29]. This suggests that these materials are useful for nonlinear optical applications.

4. Conclusions

This paper deals with the preparation of ZnO and Ga-doped ZnO films by spin-coating technique on a glass substrate. The XRD and Raman studies indicated that these films possess amorphous nature. The decline in the grain size is observed from the AFM images, which affects the film's optical properties. The high transmittance of the pure and Ga-doped ZnO film are around 90%, in which can be used in optoelectronic devices, and the lower values of dielectric constant 4.03–4.50 make them more efficient. The bandgap values are decreasing with increasing doping concentration. The Kramers-Kronig equations are used to calculate the linear and nonlinear optical parameters with high accuracy. The obtained n, k values for pure and Ga: ZnO thin films are varying from 2.04 to 2.15, 0.94 to 1.05, respectively, indicates the quality of the studied thin films. Furthermore, the nonlinear optical constants were also calculated. The $\chi^{(1)}$ and $\chi^{(3)}$ are varying in the range of 0.288–0.252 and 1.1×10^{-12} esu to 7×10^{-13} esu, respectively. Similarly, the nonlinear refractive index varies in the range of 1.92×10^{-11} esu to 1.30×10^{-11} esu. The observed values of nonlinear optical

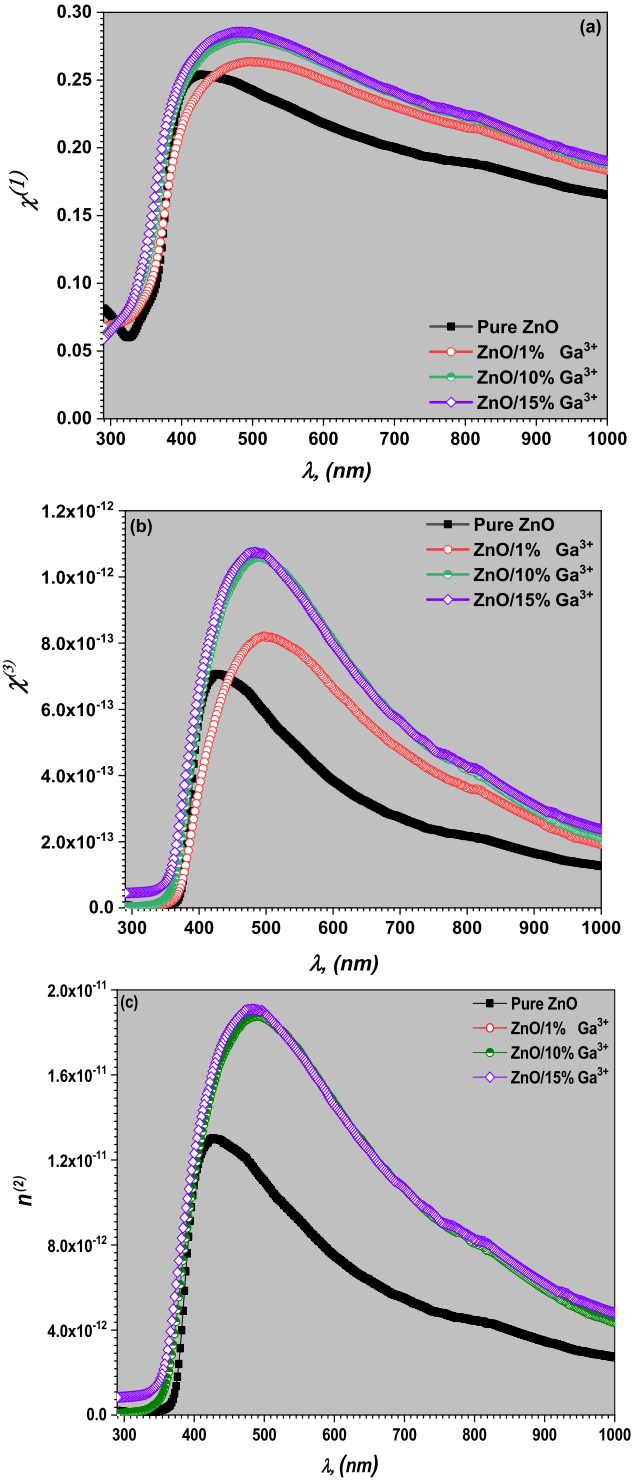

Fig. 10. (a-c). The variation of $\chi^{(1)}$, $\chi^{(3)}$ and $n^{(2)}$ as a function of wavelength for pure and Ga: ZnO nanostructured thin films.

parameters are quite higher than earlier reported data. Thus, the obtained results showed that the Ga-doped ZnO nanostructured films can be useful for the fabrication of optoelectronic devices.

Declaration of Competing Interest

The authors declare that they have no known competing financial interests or personal relationships that could have appeared to influence the work reported in this paper.

Acknowledgments

The authors extend their appreciation to the Deanship of Scientific Research at King Khalid University for funding this work through research groups program under grant number R.G.P. 2/50/40.

References

[1] Ling Zhu, Wen Zeng, Sens. Actuators, A 267 (2017) 242–261.
[2] Fei Ding, Fu. Zhengwen, Qizong Qinz, Electrochem. Solid State lett. 2 (1999) 418–419.
[3] P. Krongarrom, S.T. Rattanachan, T. Fangsuwannarak, Eng. J. 3 (2012) 60–70.
[4] J. Löffler, R. Groenen, J.L. Linden, M.C.M. Van de Sanden, R.E.I. Schropp, Thin Solid Films 392 (2001) 315–319.
[5] J. Owen, M.S. Son, K.H. Yoo, B.D. Ahn, S.Y. Lee, Appl. Phys. Lett. 90 (2007) 033512.
[6] X. Wang, Y. Ding, Z. Li, J. Song, Z.L. Wang, J. Phys. Chem. C 113 (2009) 1791–1794.
[7] V. Figà, J. Luc, B. Kulyk, M. Baitoul, B. Sahraoui, J. Eur. Optical Soc. - Rapid Publ. 4 (2009) 09016.
[8] T. Makino, C.H. Chia, Y. Segawa, M. Kawasaki, A. Ohtomo, K. Tamura, Y. Matsumoto, H. Koinuma, Appl. Surf. Sci. 189 (2002) 277–283.
[9] M. Zamfirescu, A. Kavokin, B. Gil, G. Malpuech, M. Kaliteevski, Phys. Rev. B 65 (2002) 161205.
[10] V. Bhosle, A. Tiwari, J. Narayan, J. Appl. Phys. 100 (2006) 033713.
[11] A. Ashour, M.A. Kaid, N.Z. El-Sayed, A.A. Ibrahim, Appl. Surf. Sci. 252 (2006) 7844–7848.
[12] C.M. Muiva, T.S. Sathiaraj, K. Maabong, Ceram Int. J. 37 (2011) 555–560.
[13] A.G. Cuevas, K. Balangcod, T. Balangcod, A. Jasmine, Procedia Eng. 68 (2013) 537–543.
[14] M. Ali, J. Basrah Res. 37 (2011) 49–56.
[15] X. Pan, Z. Ye, J. Li, G. Xiuquan, Y. Zeng, H. He, L. Zhu, Y. Che, Appl. Surf. Sci. 253 (2007) 5067–5069.
[16] X.L. Chen, B.H. Xu, J.M. Xue, Y. Zhao, C.C. Wei, J. Sun, Y. Wang, X.D. Zhang, X. H. Geng, Thin Solid Films 515 (2007) 3753–3759.
[17] H. Kato, M. Sano, K. Miyamoto, T. Yao, J. Cryst. Growth 237 (2002) 538–543.
[18] A.S. Juareza, A.T. Silverb, A. Ortizc, E.P. Zironid, J. Rickards, Thin Solid Films 333 (1998) 196–202.
[19] A. Kharatzade, F.J. Sheini, R. Yousef, Mater. Des. 107 (2016) 47–55.
[20] S. Fernándeza, J. Grandalb, A. Trampertb, F.B. Naranjoc, Mater. Sci. Semicond. Process. 63 (2017) 115–121.
[21] S.B. Zhang, S.h. Wei, A. Zunger, Phy. Rev. B 63 (2001) 075205–075210.
[22] Chris G. Van de Walle, Hydrogen as a cause of doping in zinc oxide, Phys. Rev. Lett. 85 (5) (2000) 1012–1015, https://doi.org/10.1103/PhysRevLett.85.1012.
[23] S.S. Shinde, K.Y. Rajpure, Appl. Surf. Sci. 257 (2011) 9595–9599.
[24] Reza Ebrahimifard, Mohammad Reza Golobostanfard, Hossein Abdizadeh, Appl. Surf. Sci. 290 (2014) 252–259.
[25] Ha-Rim. An, HyO-Jin Ahn. Jeong-Woo Park, Ceram. Int. 41 (2015) 2253-2259.
[26] J.A. Sans, J.F. Sanchez-Royo, A. Segura, Superlattices Microstruct. 43 (2008) 362–367.
[27] M. Aslam Manthrammel, A.M. Aboraiab, I.S. Mohd Shkir, Mohammed A. Yahia, H. Y. Assiri, V. Zahrana, S. AlFaify Ganesh, Alexander V. Soldatov, Opt. Laser Technol. 112 (2019) 207–214.
[28] S. Chen, N. Noor, I.P. Parkin, R. Binions, J. Mater. Chem. A 2 (2014) 17174–17182.
[29] A.A.A. Darwisha, A.M. Aboraia, Alexander V. Soldatov, I.S. Yahia, Opt. Mater. 95 (2019) 109219.
[30] K. Deva Arun Kumar, S. Valanarasu, V. Ganesh, Mohd. Shkir, A. Kathalingam, S. AlFifay, J. Electronic Mater. 47 (2018) 1335–1343.
[31] N. Ashkenov, B.N. Mbenkum, C. Bundesmann, V. Riede, M. Lorenz, D. Spemann, E. M. Kaidashev, A. Kasic, M. Schubert, M. Grundmann, G. Wagner, J. Appl. Phys. 93 (2003) 126–133.
[32] N. Hasuike, H. Fukumura, H. Harima, K. Kisoda, H. Matsui, H. Saeki, H. Tabata, 16 (2004) S5807-S5810.
[33] V. Ganesh, L. Haritha, Mohd. Anis, Mohd Shkir, I.S. Yahia, Arun Singh, S. AlFaify, Solid State Sci. 86 (2018) 98–106.
[34] S. AlFaify, V. Ganesh, L. Haritha, Mohd Shkir, Phys. B: Condens. Matter 562 (2019) 135–140.
[35] S. Scheel, L. Knoll, D.G. Welsch, Phys. Rev. A 60 (1999) 4094.
[36] M.M. El-Nahass, K.F. Abd-El-Rahman, A.M.M. Farag, A.A.A. Darwish, Int. J. Mod. Phys. 18 (2004) 421–434.
[37] M. Sesha Reddy, K.T. Ramakrishna Reddy, B.S. Naidu, P.J. Reddy, Opt. Mater. 4 (1995) 787-790.
[38] M. Frumar, J. Jedelsky, B. Frumarova, T. Wagner, M. Hrdlicka, J. Non Cryst. Solids 326 (2003) 399–404.
[39] H. Ticha, L. Tichy, J. Optoelectron. Adv. Matter. 4 (2002) 381–386.
[40] C.C. Wang, Phys. Rev. B. 2 (1970) 2045.
[41] J. Wynne, Phys. Rev. 178 (1969) 1295.
[42] H. Nasu, J.D. Mackenzie, Opt. Eng. 26 (1987) 262102.